AIP | Applied Physics Letters

Negative refraction and partial focusing with a crossed wire mesh: Physical insights and experimental verification

Tiago A. Morgado, João S. Marcos, Stanislav I. Maslovski, and Mário G. Silveirinha

Citation: Appl. Phys. Lett. **101**, 021104 (2012); doi: 10.1063/1.4734510

View online: http://dx.doi.org/10.1063/1.4734510

View Table of Contents: http://apl.aip.org/resource/1/APPLAB/v101/i2

Published by the American Institute of Physics.

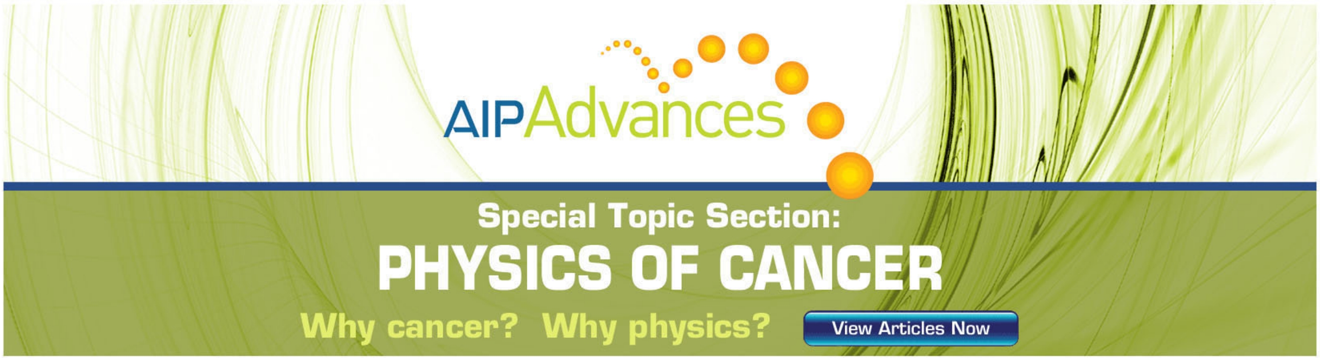

APPLIED PHYSICS LETTERS **101**, 021104 (2012)

Negative refraction and partial focusing with a crossed wire mesh: Physical insights and experimental verification

Tiago A. Morgado, João S. Marcos, Stanislav I. Maslovski, and Mário G. Silveirinha[a]
Universidade de Coimbra, Instituto de Telecomunicações, Departamento de Engenharia Electrotécnica,
Pólo II, 3030 Coimbra, Portugal

(Received 23 May 2012; accepted 23 June 2012; published online 10 July 2012)

We experimentally verify that a flat metamaterial lens formed by nonconnected crossed metallic wires enables the partial focusing of electromagnetic waves, as a consequence of the phenomenon of all-angle broadband negative refraction in such media. We prove that the strength of the negative refraction effect can be controlled by adjusting the angle between the crossed wires. © *2012 American Institute of Physics*. [http://dx.doi.org/10.1063/1.4734510]

Negative refraction has been in the limelight in recent years because it challenges the common perception of the refraction phenomenon. A beam of light incident on the surface of a material exhibiting negative refraction is bent in an unusual manner, so that the incident and refracted rays appear on the same side with respect to the normal direction in the plane of incidence. Perhaps the most interesting consequence of this anomalous refraction effect is the possibility of focusing a divergent beam of rays using simply a planar slab.

The phenomenon of negative refraction may be observed, for instance, in materials with simultaneously negative permittivity and permeability (negative index of refraction), as originally predicted by Veselago[1] and later developed by Pendry.[2] It can also be based on photonic crystals with engineered dispersion[3,4] and on hyperbolic media[5–12] such that the principal components of either the permittivity tensor or permeability tensor have opposite signs. However, there are still other possibilities. In particular, in Ref. 13 a distinct route for all-angle broadband negative refraction was put forward. This approach relies on the spatially dispersive (nonlocal) response and waveguiding properties of a metamaterial formed by nonconnected crossed metallic wires (Fig. 1).[13,14] The effect of negative refraction in this metamaterial can be understood by noting that each set of parallel wires determines a separate propagation channel, such that the wave is guided along the direction of the wires.[13] The orientation of the incoming electric field determines which set of wires is excited. For example, for the geometry of Fig. 1, the dominant channel of propagation is the one associated with the wires parallel to the $\hat{\mathbf{u}}_1$ direction, because the incoming electric field is nearly parallel to $\hat{\mathbf{u}}_1$. Thus, the energy flow direction associated with the refracted wave should be roughly parallel to $\hat{\mathbf{u}}_1$, and this implies a negative refraction. Based on these ideas, in Ref. 15 we have analytically demonstrated the partial focusing of electromagnetic waves using a planar metamaterial lens. The objective of this work is to confirm experimentally this partial focusing effect as well as to give further physical insights into the phenomenon of negative refraction in the crossed wire mesh metamaterial.

To this end, a quasi-planar prototype of the crossed wires lens was designed to operate at microwave frequencies (3.5 GHz) and was fabricated using a layer by layer design and printed circuit board (PCB) techniques (Fig. 2). In this design, the cylindrical metallic wires are replaced by metallic strips. The geometry of the lens is illustrated in Fig. 2(a). It is formed by four PCBs of thickness $a/2 = 1.27$ mm and two PCBs of thickness $a/4 = 0.635$ mm of RT/DUROID 6010LM with dielectric constant $\varepsilon_{\mathrm{h}} = 10.2$ and loss tangent $\tan\delta = 0.0023$. The metallic strips are printed in the four thicker boards (thickness $a/2$) and are tilted by ±45° with respect to the z-direction, such that the metallic strips in adjacent boards are mutually orthogonal. The width of the metallic strips is $w_s = 0.4$ mm, the lattice constant is $a = 2 \times 1.27 = 2.54$ mm, the width of the lens along the x-direction is $W \approx 71.25\sqrt{2}a = 256$ mm, and the depth of the lens along the z-direction is $L = 50a = 127$ mm. A very short balanced printed dipole-type antenna (see zoom-in inset in Fig. 2(a)) with length $l = \lambda_0/(4\sqrt{\varepsilon_{\mathrm{h}}}) \approx 7$ mm is used to excite the structure, and is placed at a distance $d_1 = 0.25L = 31.75$ mm from the first interface of the lens. Due to the high dielectric constant of the substrate, this excitation creates an electric field distribution that is mainly confined to the xoz plane, which is the condition required for the proper operation of the lens. The short dipole is printed on one of the two thinner boards (thickness $a/4$), which in turn, together with the other thinner board, is placed at the middle of the structure between the two pairs of thicker boards with mutually orthogonal printed strips. Finally, microwave absorbers (Eccosorb LS-26) were positioned at the sides of the boards to avoid reflections from the edges (see Fig. 2(b)). The y-component of the magnetic field was measured 2 mm above the lens using a near-field scanner with a round shielded loop probe connected to a vector network analyzer (R&S ZVB20).

The measured squared intensity of the y-component of the magnetic field $|H_y|^2$ is depicted in Fig. 3(a) for two different frequencies of operation around 3.5 GHz. It is manifest from Fig. 3(a) that notwithstanding the non-ideal radiation profile of the short dipole-type antenna (which is slightly asymmetric due to imperfect balanced operation),

---

[a] Author to whom correspondence should be addressed. Electronic mail: mario.silveirinha@co.it.pt.

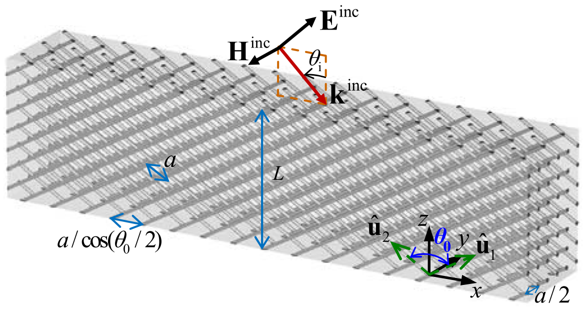

FIG. 1. Geometry of the crossed wires metamaterial with arbitrary angle between the two arrays of wires. One array of wires is oriented along the direction $\hat{\mathbf{u}}_1 = \sin(\theta_0/2)\hat{\mathbf{u}}_x + \cos(\theta_0/2)\hat{\mathbf{u}}_z$, whereas the other array is oriented along $\hat{\mathbf{u}}_2 = -\sin(\theta_0/2)\hat{\mathbf{u}}_x + \cos(\theta_0/2)\hat{\mathbf{u}}_z$. The distance between each of the adjacent sets of wires is $a/2$. The plane of incidence is the xoz plane and the incident wave is TM-z polarized.

the crossed wires lens enables the partial focusing of the incident electromagnetic radiation at two points located inside and outside the lens.

In order to confirm the experimental results, the electromagnetic response of the same setup was simulated using CST Microwave Studio[16] [Fig. 3(b)]. It can be seen that the experimental results are in good agreement with the full wave simulations. Moreover, it is worth noting that the electromagnetic field distributions are not symmetric along the x-direction in both the experimental and numerical results. Even though the imperfect radiation of the source contributes in part to this lack of symmetry, the asymmetry observed inside the lens is essentially a consequence of the finite number of planes of wires. It can be verified (not shown here) that even using a completely balanced source the asymmetry is still revealed in this finite-height lens. In particular, the inner partial focus appears slightly tilted to the right in Figs. 3(a) and 3(b) as a consequence of the metallic strips of the upper plane (where the measurement is taken) being tilted by 45° relatively to z-axis.

Despite the obvious similarities between the experimental and numerical results, there are also some slight discrepancies. These are related to fabrication imperfections, especially in the printed dipole-type antenna used as excitation source. In fact, owing to its subwavelength dimensions and fabrication complexity, the printed dipole is extremely sensitive to perturbations and, hence, is likely responsible for the slight mismatch between the experimental and numerical results. Moreover, a difficulty in our design is that a balanced operation of the short-dipole such that the dipole arms are fed with symmetric currents can only be ensured over a narrow bandwidth. The extreme sensitivity of the printed dipole and its inherently narrow-band operation preclude an estimation of the frequency bandwidth of the fabricated lens. It should be underlined, however, that it is expected that the fabricated lens may operate over a wide frequency band, as theoretically predicted in Refs. 13 and 15.

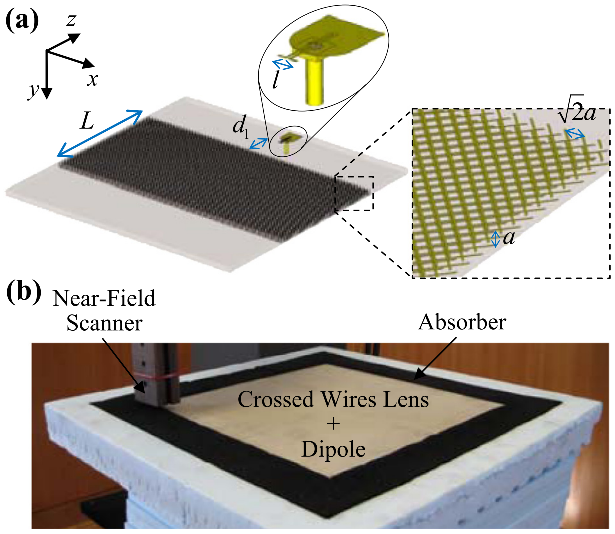

FIG. 2. (a) Geometry of the crossed wires lens. The metamaterial lens is formed by only four planes of metallic strips along the y-direction and is excited by a balanced dipole-type antenna illustrated in detail in the zoom-in view. (b) Photo of the fabricated crossed wires lens prototype.

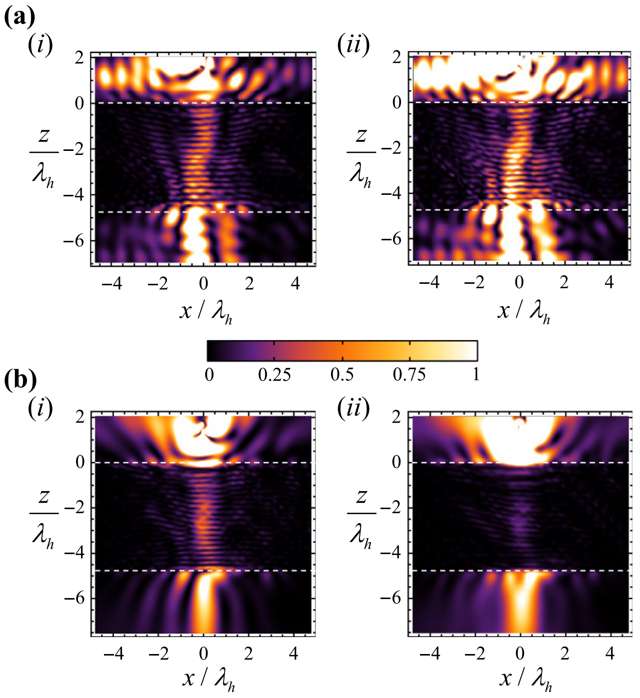

FIG. 3. (a) Experimental results of the normalized squared amplitude of the normal y-component of the magnetic field for (i) $f = 3.51$GHz, (ii) $f = 3.53$GHz. The scanning is taken 2 mm above the lens. The source is placed at $z \approx 1.2\lambda_h$. (b) (i) Normalized squared amplitude of the normal y-component of the magnetic field and (ii) normalized squared amplitude of the in-plane component of the electric field for a frequency of operation $f = 3.53$GHz, obtained with CST Microwave Studio.[16]

From the numerical results depicted in Fig. 3(b), it is also noticeable that the crossed wire mesh is a low impedance material,[13,15] since the intensity of the electric field inside the lens is weaker than outside, whereas the intensity of the magnetic field is of the same order. As a result, there is a slight impedance mismatch with the surrounding medium, perceptible in the reflections observed in the region near the first interface of the lens (see Figs. 3(a) and 3(b)).

As already mentioned in the introduction, the negative refraction in the crossed wire mesh can be intuitively understood by noting that the two sets of parallel wires behave as two concurrent channels of propagation (or waveguides) for the incoming wave, and that the transmission occurs mainly along the set of wires that is better coupled to the incoming electric field. Based on this understanding of the negative

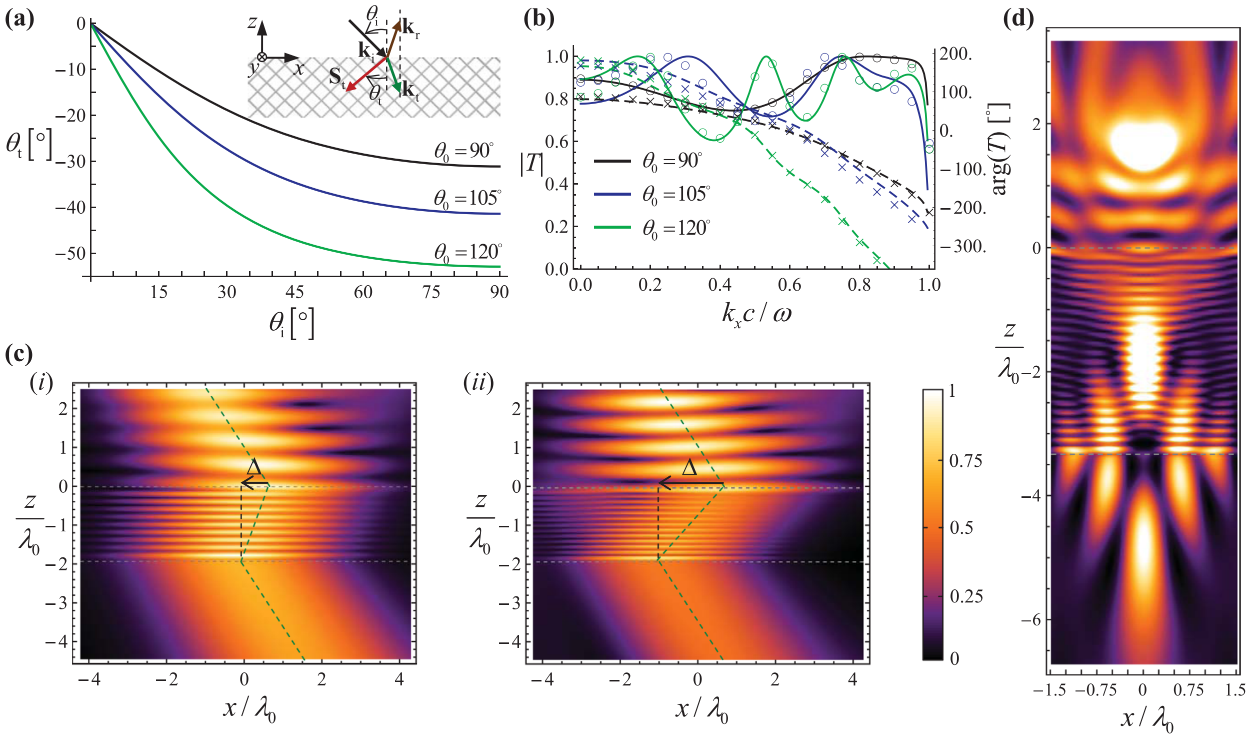

FIG. 4. (a) Angle of transmission of the energy density flux (Poynting vector) as a function of the angle of incidence for different angles θ_0 between the two arrays of wires. The normalized frequency of operation is $\omega a/c = 0.6$, the radius of the wires is $r_w = 0.05a$, and the host permittivity is $\varepsilon_h = 1$. The inset illustrates the geometry of the problem showing the incident, reflected and transmitted (refracted) waves. (b) Amplitude and phase of the transmission coefficient T as a function of the normalized k_x component of the wave vector for different angles θ_0. The thickness of the slab is $L = 25a$, and the remaining parameters are as in (a). The solid curves (continuous lines: amplitude; dashed lines: phase) correspond to the effective medium model,[15] whereas the discrete symbols (circles: amplitude; crosses: phase) correspond to full wave results.[16] (c) Normalized amplitude of the magnetic field $|\mathbf{H}|$ inside and outside the crossed wire mesh calculated using the nonlocal effective medium model. The excitation is a Gaussian beam with transverse magnetic polarization characterized by $2w_0 = 4\lambda_0$ and an incident angle of $\theta_i = 33°$ at $\omega a/c = 0.6$. The metamaterial slab is periodic along the x- and y- directions. The gray dashed lines represent the interfaces of the slab, whereas the green dashed lines represent the direction of the energy density flux. The metamaterial slab has the following structural parameters: $L = 20a$, $r_w = 0.05a$, and $\varepsilon_h = 1$. (i) $\theta_0 = 90°$; (ii) $\theta_0 = 120°$. (d) Squared (normalized) amplitude of the magnetic field $|\mathbf{H}|^2$ at the frequency of operation $\omega a/c = 0.6$, calculated using the effective medium model.[15] The metamaterial lens has the following structural parameters: $L = 35a$, $d_1 = 0.5L$, $r_w = 0.05a$, $\varepsilon_h = 1$, and $\theta_0 = 115°$.

refraction mechanism, it is natural to wonder what happens if the angle between the two sets of parallel wires is increased. Can the angle of refraction be controlled in this manner? To answer this question, in what follows we study theoretically and numerically the electromagnetic response of crossed wire mesh configurations where the angle between the two arrays of parallel wires θ_0 is different from 90° (Fig. 1), namely $\theta_0 > 90°$.

Similar to the standard nonconnected wire medium formed by two mutually orthogonal wire arrays,[13,15] the dielectric function of crossed wire mesh configurations with arbitrary angle between the two sets of wires can be obtained using effective medium methods.[17] It is possible to prove that in the general case (Fig. 1) the dielectric function of the metamaterial is given by $\bar{\bar{\varepsilon}}_{\mathrm{eff}} = \varepsilon_h[\bar{\bar{\mathbf{I}}} + (\varepsilon_{11} - 1)\hat{\mathbf{u}}_1\hat{\mathbf{u}}_1 + (\varepsilon_{22} - 1)\hat{\mathbf{u}}_2\hat{\mathbf{u}}_2]$, where ε_h is the relative permittivity of the host medium, $\bar{\bar{\mathbf{I}}}$ is the identity dyadic, $\hat{\mathbf{u}}_1 = \sin(\theta_0/2)\hat{\mathbf{u}}_x + \cos(\theta_0/2)\hat{\mathbf{u}}_z$, and $\hat{\mathbf{u}}_2 = -\sin(\theta_0/2)\hat{\mathbf{u}}_x + \cos(\theta_0/2)\hat{\mathbf{u}}_z$ are unity vectors that determine the orientation of the two sets of wires. The permittivity components ε_{11} and ε_{22} are the same as in Ref. 15. This formula generalizes the well-known permittivity tensor of a crossed wire mesh with $\theta_0 = 90°$ [see, e.g., Eq. (1) of Ref. 15].

To study the effect of tuning θ_0 on the negative refraction, we have calculated the angle of transmission θ_t of the energy density flux (Poynting vector) as a function of the angle of incidence θ_i (see inset of Fig. 4(a)), using the relation $v_g = \nabla_k \omega(\mathbf{k})$, where $\omega(\mathbf{k})$ represents the dispersion of the plane wave modes that is determined using the effective medium model. One can see from Fig. 4(a) that the angle of transmission θ_t becomes more negative as the angle θ_0 between the two sets of wires is increased. Hence, these results indicate that by changing the angle θ_0 between the two arrays of wires it is possible to boost the strength of the negative refraction in the crossed wire mesh.

To confirm these results, we have used the full wave electromagnetic simulator[16] to calculate the transmission coefficient T of crossed wire mesh configurations with different angles θ_0 under plane wave incidence (see Fig. 1). In addition, we have also calculated the transmission coefficient T using the nonlocal homogenization model, similar to what was done in Ref. 15. The results obtained using the two different methods are shown in Fig. 4(b). First, it should be stressed the very good agreement between the effective medium results and the full wave results, which demonstrates the accuracy of the analytical model. Moreover, Fig. 4(b) shows that the phase of T decreases with k_x, which based on the criterion introduced in Ref. 13 indicates the emergence of negative refraction. In particular, one can see that the slope of the curves of the phase of T increases with the angle

θ_0 between the two arrays of parallel wires, which is a clear proof that, in fact, by increasing θ_0 the negative refraction effect is enhanced. On the other hand, it is seen from Fig. 4(b) that the amplitude of the transmission coefficient deteriorates slightly for some spatial harmonics (or angles of incidence) with the increase of the angle θ_0.

In order to provide further evidence for the enhancement of the negative refraction effect in crossed wire mesh configurations with $\theta_0 > 90°$, we have used the effective medium model together with Fourier theory[12] (similar methods are reported in detail in Ref. 15) to analyze the refraction of a Gaussian beam at the interfaces of metamaterial slabs with $\theta_0 = 90°$ and $\theta_0 = 120°$ (Figs. 4c(i) and 4c(ii), respectively). Comparing Figs. 4c(i) and 4c(ii), it can be observed that the absolute value of the spatial lateral shift Δ suffered by the Gaussian beam at the interfaces of the slab increases with θ_0. Hence, based on these results we conclude that, in fact, it is possible to boost the strength of negative refraction by increasing the angle θ_0 between the two arrays of parallel wires. On the other hand, and consistent with the transmission profiles of Fig. 4(b), one can notice that the level of reflections at the first interface of the slab increases slightly for larger values of θ_0 (see Figs. 4c(i) and 4c(ii)). This is simply a consequence of the fact that the transverse permittivity of the medium (i.e., ε_{xx}) grows with the angle θ_0, which somewhat deteriorates the matching with the external medium. Despite this inconvenience, one can see that the transmission level remains satisfactory for considerably large angles (see Fig. 4c(ii)).

Following this achievement, we have investigated the focusing properties of crossed wires lenses with $\theta_0 > 90°$. In our analysis, we consider that the structured lens is illuminated by a magnetic line source infinitely extended along the y-direction. Then, using Eq. (8) of Ref. 15, we have calculated the magnetic field distribution inside and outside a lens infinitely extended along the x- and y-directions. The spatial map of the squared normalized amplitude of the magnetic field for a crossed wires lens configuration with $\theta_0 = 115°$ is shown in Fig. 4(d). It is clearly seen an intense elongated (or partial) focus of the magnetic field both inside and outside the lens. Therefore, similar to the standard crossed wires lens configuration (see Fig. 4(c) of Ref. 15), the modified geometry also enables the partial focusing of p-polarized electromagnetic radiation. Moreover, by comparing Fig. 4(d) and Fig. 4(c) of Ref. 15, one can recognize the possibilities opened by the improved lens configurations with obtuse angles θ_0, which permit obtaining a partial focusing with a significantly thinner metamaterial lens and to increase the focal depth of the lens.

In conclusion, we have experimentally verified the partial focusing of electromagnetic waves using a planar lens formed by nonconnected crossed metallic wires, taking advantage of the all-angle broadband negative refraction property.[13] By noting that the negative refraction phenomenon is rooted in the geometry of the structure that effectively provides two separate propagation channels for the incoming wave, we suggested a modification of the internal structure of the metamaterial that enables boosting the strength of the negative refraction, and provides further degrees of freedom in the design of the planar lenses.

[1] V. G. Veselago, Sov. Phys. Usp. **10**, 509 (1968).

[2] J. B. Pendry, Phys. Rev. Lett. **85**, 3966 (2000).

[3] M. Notomi, Phys. Rev. B **62**, 10696 (2000).

[4] E. Cubukcu, K. Aydin, E. Ozbay, S. Foteinopoulou, and C. M. Soukoulis, Nature (London) **423**, 604 (2003).

[5] D. R. Smith and D. Schurig, Phys. Rev. Lett. **90**, 077405 (2003).

[6] D. R. Smith, D. Schurig, J. J. Mock, P. Kolinko, and P. Rye, Appl. Phys. Lett. **84**, 2244 (2004).

[7] X. Fan, G. P. Wang, J. C. W. Lee, and C. T. Chan, Phys. Rev. Lett. **97**, 073901 (2006).

[8] A. J. Hoffman, L. Alekseyev, S. S. Howard, K. J. Franz, D. Wasserman, V. A. Podolskiy, E. E. Narimanov, D. L. Sivco, and G. Gmachl, Nat. Mater. **6**, 946 (2007).

[9] A. Fang, T. Koschny, and C. M. Soukoulis, Phys. Rev. B **79**, 245127 (2009).

[10] Y. Liu, G. Bartal, and X. Zhang, Opt. Express **16**, 15439 (2008).

[11] J. Yao, Z. Liu, Y. Liu, Y. Wang, C. Sun, G. Bartal, A. M. Stacy, and X. Zhang, Science **321**, 930 (2008).

[12] T. A. Morgado, S. I. Maslovski, and M. G. Silveirinha, New J. Phys. **14**, 063002 (2012).

[13] M. G. Silveirinha, Phys. Rev. B **79**, 153109 (2009).

[14] I. S. Nefedov, A. J. Viitanen, and S. A. Tretyakov, Phys. Rev. B **72**, 245113 (2005).

[15] T. A. Morgado and M. G. Silveirinha, Metamaterials **4**, 112 (2010).

[16] CST Microwave Studio 2010.

[17] M. G. Silveirinha, Phys. Rev. B **75**, 115104 (2007).